

NANO MICRO  
**small**

Supporting Information

for *Small*, DOI: 10.1002/smll. 201200156

Ultrafast Dynamics of Exciton Formation in Semiconductor  
Nanowires

*Chaw Keong Yong , Hannah J. Joyce , James Lloyd-  
Hughes , Qiang Gao , Hark Hoe Tan , Chennupati  
Jagadish , Michael B. Johnston , and Laura M. Herz \**

**Supporting information for: Ultrafast Dynamics of Exciton Formation in Semiconductor Nanowires**

*Chaw Keong Yong, Hannah J. Joyce, James Lloyd-Hughes, Qiang Gao, Hark Hoe Tan, Chennupati Jagadish, Michael B. Johnston, and Laura M. Herz\**

**Hot carrier relaxation in GaAs**

For non-resonant excitation, it has been shown that the average carrier cooling rate of a hot carrier at low substrate temperature ( $T_l$ ) is dominated by longitudinal optical (LO) phonon emission at high carrier temperature ( $T_e$ ) and acoustic (AC) phonon emission when the excess energy becomes lower than the LO-phonon energy.<sup>[1]</sup> The main average cooling rates  $\langle dT/dt \rangle$  (in units of K/ps) per electron in a Maxwellian distribution of temperature are given by:<sup>[1]</sup>

$$\left\langle \frac{dT_e}{dt} \right\rangle_{OP} = 3240.319 \left[ \exp\left(-\frac{E_{LO}}{KT_e}\right) - \exp\left(-\frac{E_{LO}}{KT_l}\right) \right]; \quad (1)$$

$$\left\langle \frac{dT_e}{dt} \right\rangle_{AD} = 3.1423 \times 10^{-5} T_e^{3/2} \left( \frac{T_e - T_l}{T_e} \right); \quad (2)$$

$$\left\langle \frac{dT_e}{dt} \right\rangle_{AP} = 12.134 \times 10^{-3} T_e^{1/2} \left( \frac{T_e - T_l}{T_e} \right); \quad (3)$$

where the subscripts OP, AD and AP to the average cooling rates denote the different cooling mechanisms arising from optical phonon, acoustic-deformation-potential and acoustic-piezoelectric scattering, respectively. Given the large diameter of the GaAs-CSS nanowires we reasonably took the bulk GaAs value for the LO phonon energy ( $E_{LO} = 36$  meV). The evolution of the carrier cooling in the nanowires is deduced by calculation of their average energy lost per electron-hole pair  $\langle dT_e/dt \rangle \approx \langle dE/dt \rangle$  with the variation in temperature extracted from:

$$T_e(t) = T_0 - \int_0^t \left\langle \frac{dT_e}{dt} \right\rangle dt'; \quad (4)$$

where  $T_0$  is given by the excess energy of carriers during initial excitation. The output of the numerical simulation is shown in Figure S1.

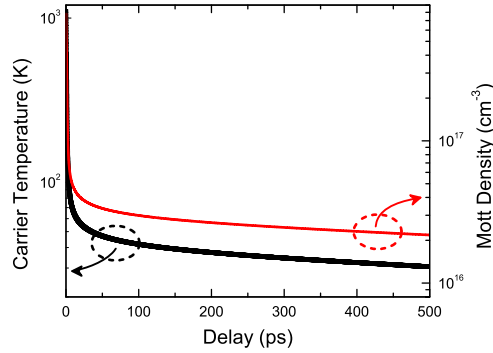


Figure S1: Left axis: Charge carrier temperature  $T_e$  in the GaAs-CSS nanowires (black line), as extracted from the calculations described in the text. Right axis: Mott transition density  $N_M$  ( $T_e$ ) (red line) extracted from Eq. (5) and shown as a function of time after excitation

### Calculation of the Mott transition density

The Mott density  $N_M$  denotes the electron-hole pair density at which the Debye-Hückel screening length ( $K_D$ ) becomes comparable to the exciton Bohr radius ( $a_b$ ), which yields:<sup>[2]</sup>

$$N_M = (1.19)^2 \frac{\epsilon_r \epsilon_0 k_B T_e}{e^2 a_b^2}, \quad (5)$$

where  $\epsilon_r$  is the dielectric constant and  $T_e$  is the charge carrier temperature. In a bulk semiconductor, excitons are expected to become unstable when the electron-hole pair density exceeds the Mott limit. We calculated the theoretical Mott density from Equation (5) using the simulated carrier temperature shown in Figure S1 and a value of  $a_b = 11$  nm for bulk GaAs.<sup>[2]</sup>

The resulting theoretical values for  $N_M$  are shown in Figure S1. Since carrier cooling is slow in GaAs due to the weak acoustic phonon coupling<sup>[1]</sup> the carrier temperature is found to be higher than the lattice temperature over the 500 ps observation window. As a result, the theoretical Mott limit evolves with time after excitation and does not fully reach the value predicted for the substrate temperature of 10 K during the observation window.

### Radiative plasma recombination

We are able to convert the measured PL emitted through electron-hole plasma recombination ( $I_{plasma}$ ) into the free electron or hole density  $n$  by taking account of the carrier temperature  $T_e$  and the density of absorbed photons as follows. For low excitation fluence,  $I_{plasma}$  is related to  $n$  via the bimolecular recombination constant  $B$  through.<sup>[3]</sup>

$$I_{plasma} = Bn^2; \quad (6)$$

Here,  $B$  is given by:

$$B = \frac{2\sqrt{\pi}n_r e^2 \hbar E_g}{m_0 c^3 [(m_e + m_h) k_B T_e]^{1.5}} \frac{E_p}{3}; \quad (7)$$

where  $E_p$  is the interband transition matrix element,  $m_e$  and  $m_h$  are the effective masses of the electron and the hole,  $E_g$  is the bandgap energy and  $n_r$  is the refractive index.<sup>[3]</sup>

Since out of all parameters contained in  $B$  only the free-carrier temperature  $T_e$  varies with time, the carrier population  $n$  is obtained from the plasma emission normalized to its initial ( $t = 0$ ) value, i.e.  $I_{plasma}/I_0$ , through:

$$n = n_o \sqrt{\frac{I_{plasma} T_e^{1.5}}{I_o T_o^{1.5}}}; \quad (8)$$

The initial carrier density ( $n_o$ ) immediately after photoexcitation ( $t = 0$ ) can then be calculated from the density of absorbed photons. For the case of the samples under investigation, the nanowires of diameter  $d = 50$  nm were dispersed lying flat on the substrate. The optical absorption coefficient  $a$  at the excitation energy of  $E_{photon} = 1.68$  eV is taken from literature values<sup>[4-6]</sup> at 10 K to be  $18000 \text{ cm}^{-1}$ . The sample is therefore optically thin (i.e.  $ad = 0.09$ ) resulting in the generation of a homogeneous initial carrier density  $n_o$  throughout each individual nanowire given by:

$$n_o = \frac{f_o}{E_{photon}} \times \alpha(1 - R); \quad (9)$$

Here  $f_o$  is the initial excitation pulse fluence incident on the nanowire and  $R$  accounts for the reflection losses occurred at the GaAs interface, given by  $R = (n_r - 1)^2 / (n_r + 1)^2 \approx 0.33$  with  $n_r = 3.72$ .<sup>[6]</sup>

The initial excitation fluence  $f_o$  experienced by the nanowires is given by that at the very centre of the Gaussian excitation spot profile because of the experimental conditions used, as described in the following. The excitation spot on the sample had a full-width-at-half maximum of  $w = 240$  mm, which generated emission that was imaged with two off-axis parabolic mirrors onto the nonlinear crystal with a magnification ratio of 4.1. The PL image of 1 mm diameter was then optically gated with a gate beam of 80 mm diameter. Therefore, this set-up probes an excitation area of diameter only  $0.08w$  with respect to the overall excitation

spot. The probed emission as a result is highly homogenous as it is generated by the fluence  $f_o$  at the very centre of the Gaussian excitation spot given by,

$$f_o = \frac{\sqrt{2}P}{\pi\left(\frac{W}{2}\right)^2} r_{rep}; \quad (10)$$

where  $P$  is the time-averaged total excitation power incident on the sample surface and  $r_{rep}=82\text{MHz}$  is the pulse repetition rate of the excitation laser. Overall, this system of measurement therefore ensures that a well-defined and uniform volume density of carriers is generated in the ensemble of nanowires probed.

### **Bimolecular exciton formation constant**

To account for the bimolecular exciton formation via LO and AC phonon coupling in the numerical simulations described in the main text we incorporated the functional dependence on the charge carrier temperature  $T_e$  as described by Piermarocchi et al.<sup>[7]</sup> These authors showed that the bimolecular exciton formation constant  $C$  has a contribution arising from LO-phonon coupling given by an exponential dependence on an activation energy of  $(E_{LO} - E_b)$  where  $E_{LO}$  is the LO-phonon energy and  $E_b$  is the exciton binding energy. The second component of  $C$ , related to AC-phonon coupling, was found to be fairly constant with carrier temperature.<sup>[7]</sup> We therefore use the following dependence of the bimolecular exciton formation coefficient on charge carrier temperature  $T_e$ :

$$C = C_{LO} \exp\left(-\frac{E_{LO}-E_b}{k_B T_e}\right) + C_{AC}; \quad (11)$$

Here,  $T_e$  is taken from the calculations described above and  $C_{LO}$  and  $C_{AC}$  are left as free parameters in the fits to allow for modifications due to the limited quantum confinement in the nanowires. Best fits to the data (as shown in Figure 3 of the main text) were obtained for  $C_{LO} = 2.61 \times 10^{-18} \text{ cm}^3 \text{ ps}^{-1}$  and  $C_{AC} = 1.16 \times 10^{-18} \text{ cm}^3 \text{ ps}^{-1}$ .

### Excitonic PL decay at long times after excitation

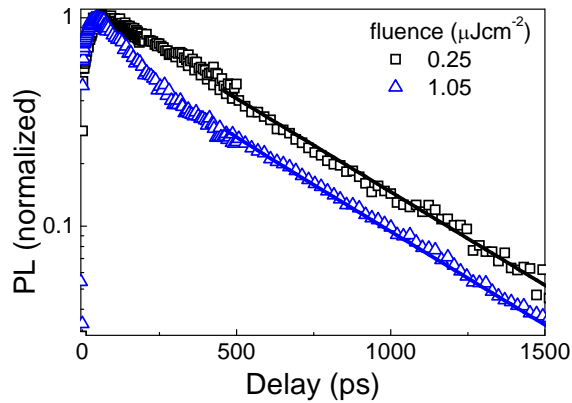


Figure S2: Normalized PL transients of GaAs CSS-NWs measured at the emission energy of the exciton (1.52 eV) for two different fluences. The short-term PL dynamics ( $\leq 500$  ps) was measured using the PL up-conversion technique, as described in the main text, while the long-term emission was measured using TCSPC. Solid lines are mono-exponentials with decay time of 420 ps.

To determine the excitonic recombination lifetime in GaAs CSS-NWs, we measured the excitonic PL using a time-correlated single-photon counting (TCSPC) system with a temporal resolution of 180 ps. The excitation and PL collimation conditions were identical to those described in the Experimental Section of the main paper. However, detection was carried out using a peltier-cooled photomultiplier tube fed into Becker & Hickl TCSPC electronics to obtain electronically gated PL decay curves. Figure S2 shows a fusion of these TCSPC data (for times  $> 500$  ps) with those obtained from PL upconversion spectroscopy (shown for times

< 500 ps) analyzed in the main paper. We find that the excitonic PL at a long time after non-resonant excitation exhibits a monoexponential decay with the decay rate independent on the excitation fluence. We thus extract the exciton lifetime ( $\tau_{NW}$ ) from a single exponential fits to the long-delay data and find a value of  $\tau_{NW} = 420$ ps.

### **Time-resolved PL measurements of bare GaAs NWs**

We here compare the exciton formation dynamics observed in GaAs-CSS nanowires with those obtained for “bare” GaAs nanowires for which no additional over-coating with higher-band-gap material had been performed. As we have shown previously,<sup>[8]</sup> the GaAs-CSS nanowires exhibit a 82% lower charge-trap density than the bare GaAs NWs. In agreement with these results, we find here that the PL of bare GaAs NWs at 10K is short-lived and dominated by fast charge trapping (see Figure S3). We fitted the model solutions described in the main text to the transient exciton and charge densities using the same parameters as for the GaAs-CSS NWs, with the exception of  $\tau_{NW}$  and  $\tau_{nr}$  which were allowed to vary. Good agreement was obtained between fits and data for  $\tau_{NW} = 6$  ps and  $\tau_{nr} = 6$  ps, as shown in Figure S3. The short lifetimes and the lack of a discernable delayed rise in the exciton density with time after excitation demonstrate that fast trapping of the electron-hole plasma sets a short time window for exciton formation and thus dominates the overall time evolution of the exciton and charge densities.



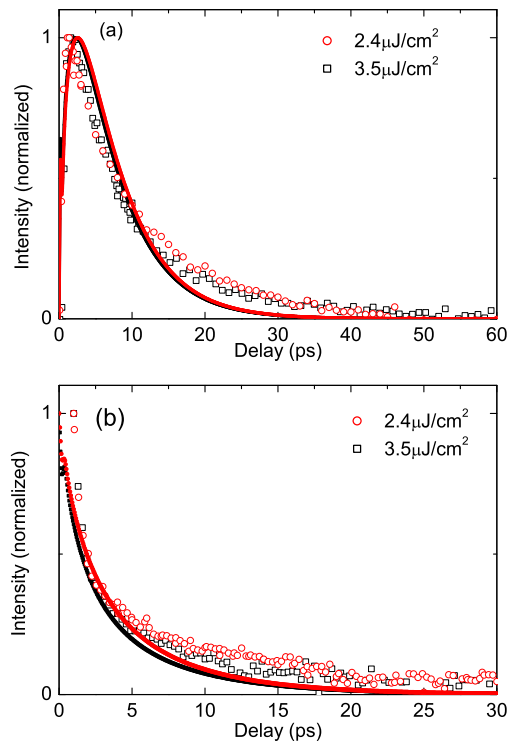


Figure S3: (a) Normalized PL transients of bare GaAs NWs measured at the emission energy of the exciton at 1.52 eV for different fluences (open symbols) along with the output of the numerical model (solid-line, as described in text). (b) Normalized free-carrier density decay for bare GaAs NWs. The data are obtained by normalizing the radiative plasma emission measured at 1.55 eV with  $T_e$ , as described in the text.

## References

- [1] R. Ulbrich, *Phys. Rev. B* **1973**, 8, 5719.
- [2] C. Klingshirn, *Semiconductor Optics*; Springer-Verlag: Berlin Heidelberg, **1997**.
- [3] J.S. Im, A. Moritz, F. Steuber, V. Harle, F. Scholz, A. Hangleiter, *Appl. Phys. Lett.* **1997**, 70, 631.
- [4] D.D. Sell, H.C.J. Casey, *Appl. Phys.* **1974**, 45, 800.

- [5] M.D. Sturge, *Phys. Rev.* **1962**, *127*, 768.
- [6] J.S.J. Blakemore, *Appl. Phys.* **1982**, *53*, R123.
- [7] C. Piermarocchi, F. Tassone, V. Savona, A. Quattropani, P. Schwendimann, *Phys. Rev. B* **1997**, *55*, 1333.
- [8] P. Parkinson, H.J. Joyce, Q. Gao, H.H. Tan, X. Zhang, J. Zou, C. Jagadish, L.M. Herz, M.B. Johnston, *Nano Lett.* **2009**, *9*, 3349.